Journal of Materials Chemistry A

Accepted Manuscript

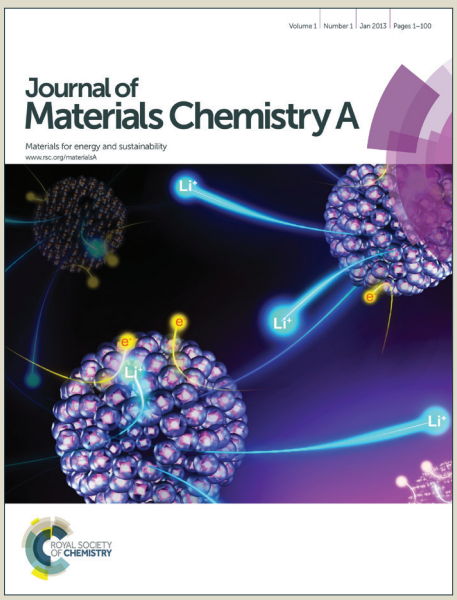

ROYAL SOCIETY OF CHEMISTRY

www.rsc.org/materialsA

Journal of Materials Chemistry A

RSCPublishing

ARTICLE

Double D-π-A Branched Organic Dye Isomers for Dye-Sensitized Solar Cells

Cite this: DOI: 10.1039/x0xx00000x

Shenghui Jiang,[a] Suhua Fan,[a,b] Xuefeng Lu,[a] Gang Zhou,[a,*] and Zhong-Sheng Wang[a,*]

Received 00th January 2012,
Accepted 00th January 2012

DOI: 10.1039/x0xx00000x

www.rsc.org/

Three double D-π-A branched organic dye isomers (**D1**, **D2**, and **D3**) with octyloxy bridge linked at different positions of the π-bridge in the D-π-A branch have been designed and synthesized for dye-sensitized solar cells (DSSCs). Their photophysical, electrochemical, and photovoltaic properties are further investigated. As compared with the reference dye isomers containing single D-π-A branch, the double D-π-A branched dye isomers consisting of two separated light-harvesting moieties in one molecule are beneficial to photocurrent generation. Moreover, the cross structure of the double D-π-A branched organic dye isomers is superior to the rod structure of the dye isomers with single D-π-A branch in suppression of the intermolecular interactions, which results in the reduced charge recombination rates in the DSSCs based on double branched organic dye isomers. Therefore, in comparison to the DSSCs based on the isomeric dyes with single D-π-A branch, the DSSCs based on double branched organic dye isomers display both improved short-circuit current and open-circuit voltage. Furthermore, similar to the single D-π-A branched organic dye isomers, those isomeric dyes with double D-π-A branches exhibit slightly different photophysical properties, which results in their varied photovoltaic performance. A highest power conversion efficiency of 8.1% and 6.9%, respectively, is achieved for isomer **D1** based DSSC with liquid and quasi-solid-state electrolyte under simulated AM1.5G solar irradiation (100 mW cm^{-2}).

Introduction

Dye-sensitized solar cells (DSSCs) have attracted extensive attention in the last two decades since the breakthrough by Grätzel and co-workers.[1] The key component of this solar cell is a photoanode which consists of a mesoporous nanocrystalline TiO_2 film covered by a monolayer of photosensitizing dye. Absorption of sunlight by the sensitizer creates a high energy state that can inject the photoexcited electrons into the conduction band of TiO_2. The oxidized dye is subsequently reduced back to the ground state by a redox system. Up to date, DSSC devices employing zinc-porphyrin dye system have shown an efficiency record of 12.3% under standard global air mass 1.5.[2] However, in view of cost and limited availability, alternative metal-free organic sensitizers[3] have also attracted considerable attention for practical applications owing to their unique advantages, such as facile structure tuning, high molar extinction coefficients, variety of optoelectronic properties and environmentally friendly. Recently, the performance of organic dye based DSSCs has been remarkably improved and impressive efficiencies over 11% have been achieved.[4]

Most of efficient organic sensitizers have donor-π bridge-acceptor (D-π-A) structures. Despite the promising results obtained so far, many metal-free organic dyes with a rod-like configuration may cause undesirable dye aggregation and charger combination. The close π-π stacking of dye molecules can lead to self-quenching of excited states and hence insufficient electron injection. Therefore, the suppression of dye aggregation is of vital importance for minimizing the charge recombination and achieving photovoltage improvements. To control the π-stacked aggregation of organic dye molecules and related charge recombination processes, several kinds of additives, such as deoxycholic acid (DCA),[5] have been physically introduced to coadsorb onto the semiconductor surface to prevent the intermolecular interactions. An alternative strategy to solve this problem is the chemical incorporation of long alkyl chains into the organic dye skeleton, which may suppress the molecular aggregation and thus improve the DSSC performance.[6] Recently, the construction of double D-π-A branched organic dyes has proved to be an effective method to reduce intermolecular interactions, retard charge recombination rate and therefore enhance the V_{oc} parameter.[7] Recently, Fungo et al. developed a double D-π-A branched sensitizer bridged by a spirofluorene with two anchoring groups separated at a distance of 10.05 Å.[8] Wang et al. investigated a series of organic sensitizers containing symmetric and asymmetric double D-π-A branches connected by flexible chains with different length.[9] We have also reported organic sensitizers with conjugated spacer bridging double D-π-A or D-π-A-π-A branches.[10]

In this article, three simple double D-π-A branched sensitizer isomers (**D1**, **D2**, and **D3**, Fig. 1) with bridge substituted at different positions are designed and synthesized. According to

previously reported research work, octyl group is sufficient to weaken the intermolecular interactions among the organic dye molecules. Therefore, an octyloxy bridge is utilized to link the two D-π-A branches. To verify the isomeric structures and fully compare the different behavior between single and double D-π-A branched organic dyes, corresponding single D-π-A branched organic dyes (**S1** and **S2**, Fig. 1) are also synthesized. According to our previous study,[11] when the alkyl groups are substituted at different position of the π-conjugated spacer for the organic dye isomers, the related photophysical and photovoltaic properties are significantly varied. Herein, for both single and double D-π-A branched organic dyes, slightly different photophysical properties can be found for related dye isomers, which results in their varied photovoltaic performance. Most importantly, in comparison to the single D-π-A branched organic dye isomers with rod-shape, the double D-π-A branched organic dye isomers possess crossed chemical structures, which is favorable for minimizing the intermolecular interaction and reducing the charge recombination in the DSSC. Therefore, the DSSCs based on the double D-π-A branched dye isomers exhibit both higher V_{oc} and short-circuit current (J_{sc}) as compared with the DSSCs based on the organic dyes with single D-π-A branch. A highest power conversion efficiency (η) of 8.1% and 6.9%, respectively, is achieved for isomer **D1** based DSSC with liquid and quasi-solid-state electrolyte.

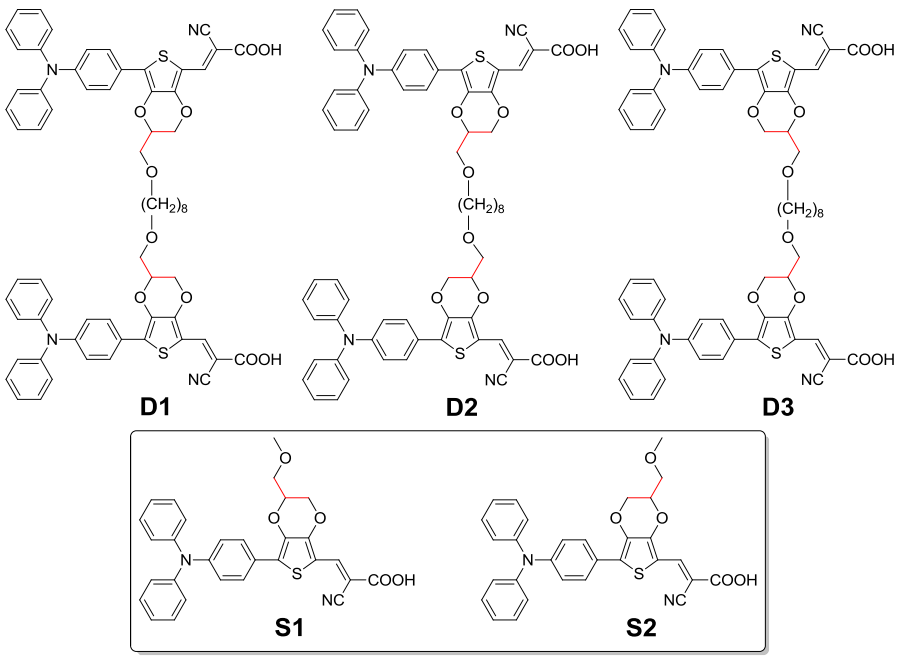

Fig. 1 Chemical structures of dye isomers **D1**, **D2**, and **D3**, and reference dye isomers **S1** and **S2**.

Experimental Section

Materials and Reagents. 1,8-Dibromooctane, *N*-bromosuccinimide (NBS) were purchased from J&K Chemical Ltd, China. Organic solvents used in this work were purified using the standard process. Other chemicals and reagents were used as received from commercial sources without further purification. Transparent conductive glass (F-doped SnO_2, FTO, 15 Ω smittance of 80%, Nippon Sheet Glass Co., Japan) was used as the substrate for the fabrication of TiO_2 thin film electrode.

Synthesis of 1,8-bis((2,3-dihydrothieno[3,4-*b*][1,4]dioxin-2-yl)methoxy)octane (2). Under argon atmosphere, sodium hydride (0.59g, 14.7 mmol), and THF (20 mL) were placed in a 100 mL three-necked flask. Then 2,3-dihydrothieno[3,4-*b*]-l,4-dioxin-2-yl methanol (2.53g, 14.7 mmol) in 20 mL THF solution was added dropwise to the reaction at 0 °C. After stirring for 1 h, 1.99 g (7.3 mmol) of 1,8–dibromooctane was inject via a syringe into the flask. The mixture was heated to reflux and stirred overnight. After cooling the reaction mixture to room temperature, the mixture was extracted with dichloromethane (DCM) twice and the combined organic phase was washed with brine and then concentrated to obtain the crude compound **2**. Further purification was carried out by column chromatography on silica gel using hexane/DCM (v/v = 2/1) as the eluent to obtain pure compound **2** as white solid, yield 72% (2.39 g). ^{1}H NMR (400 MHz, $CDCl_3$): δ ppm 6.33 (d, J = 3.6 Hz, 2H, thiophene-2), 6.32 (d, J = 3.6 Hz, 2H, thiophene-5), 4.38–4.18 (m, 4H), 4.05 (dd, J = 11.6, 7.5 Hz, 2H), 3.64 (m, 4H), 3.48 (t, J = 6.6 Hz, 4H), 3.40 (t, J = 6.8 Hz, 4H), 1.91 – 1.78 (m, 4H), 1.60 – 1.55 (m, 4H), 1.41 (m, 4H). ^{13}C NMR (100 MHz, $CDCl_3$): δ ppm 141.79, 99.91, 99.79, 72.86, 72.23, 69.33, 66.46, 34.29, 33.00, 29.70, 29.45, 28.92, 28.32, 26.15.

Synthesis of compounds 3a, 3b, and 3c. Under argon atmosphere, compound **2** (0.40 g, 0.88 mmol), *N*,*N*-dimethylformamide (DMF, 0.128g, 1.76 mmol,) and DCM (40 mL) were placed in a 100 mL three-necked flask and cooled to 0 °C. After adding $POCl_3$ (0.27 g, 1.76 mmol) via a syringe, the mixture was heated to reflux for 24 h. Then the reaction mixture was cooled to room temperature and quenched with 10% NaOAc aqueous solution (30 mL). The mixture was extracted with DCM twice and the combined organic phase was washed with brine and then concentrated. The crude product was purified by column chromatography on silica gel with hexane/DCM (v/v = 1/1) as eluent to remove other by-products. The obtained isomer mixture of compounds **3a**, **3b** and **3c** was directly used for the next step.

Synthesis of compounds 4a, 4b, and 4c. The isomer mixture of compounds **3a**, **3b**, and **3c** (306 mg, 0.60 mmol), $Pd(OAc)_2$ (2.8 mg, 2 mol%, 0.012 mmol), PCy_3HBF_4 (8.8 mg, 4mol%, 0.024 mmol), pivalic acid (18.4 mg, 30 mol%, 0.18 mmol) and K_2CO_3 (209 mg, 1.5 mmol) were placed in a Schlenk tube. The tube was purged with argon and then 4-bromo-*N*,*N*-diphenylaniline (505 mg, 2.6 equiv, 1.56 mmol) in 2 mL toluene solution was added. The reaction mixture was vigorously stirred at 110 °C for 24 h. Then the solution was cooled to room temperature, diluted with DCM，and washed with brine. The organic phase were combined, dried over $MgSO_4$ and evaporated under reduced pressure. The crude product was purified by silica gel column chromatography with hexane/DCM (v/v = 1/1) as eluent to produce pure compounds **4a** (126 mg), **4b** (115 mg) and **4c** (96 mg).

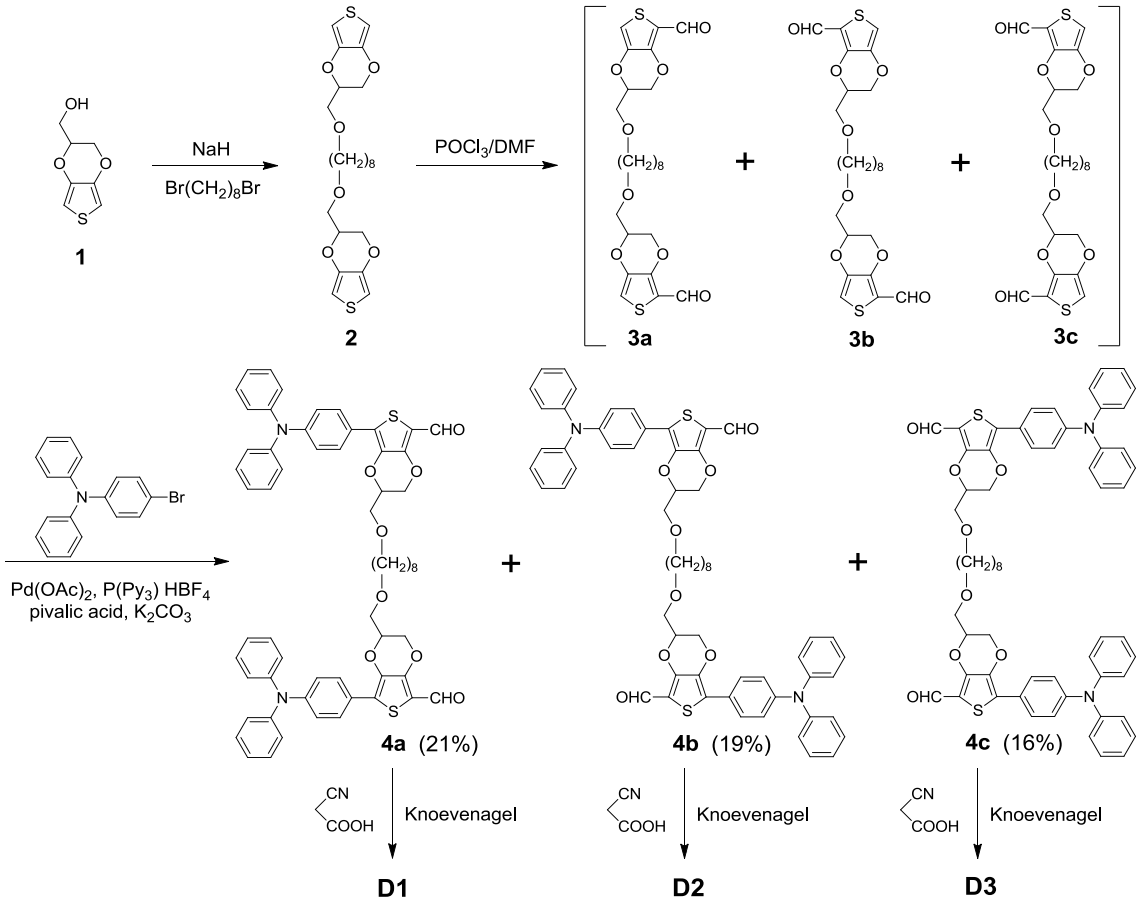

Scheme 1 Synthetic routes for dye isomers **D1**, **D2**, and **D3**.

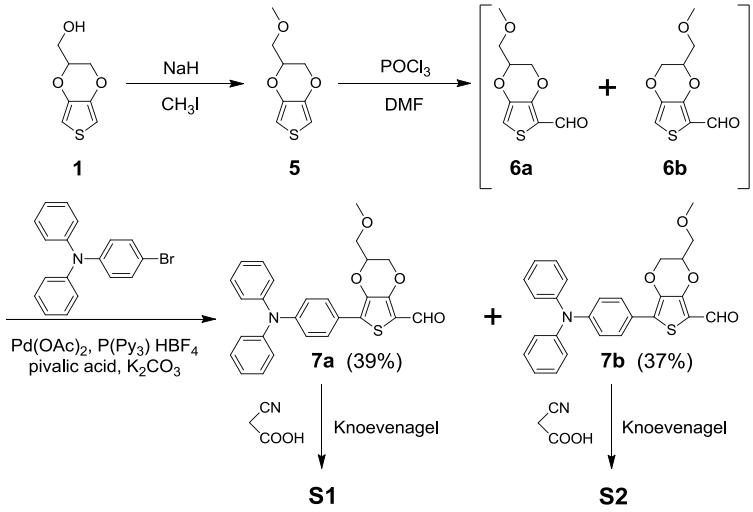

Scheme 2 Synthetic routes for reference dye isomers **S1** and **S2**.

2,2'-((Octane-1,6-diylbis(oxy))bis(methylene))bis(7-(4-(diphenylamino)phenyl)-2,3-dihydrothieno[3,4-*b*][1,4]dioxine-5-carbaldehyde) (4a). ^{1}H NMR (400 MHz, DMSO-d_6): δ ppm 9.82 (s, 2H), 7.65 (d, J = 8.7 Hz, 4H), 7.33 (t, J = 7.8 Hz, 8H), 7.15 – 7.02 (m, 12H), 6.95 (d, J = 8.7 Hz, 4H), 4.63 (d, J = 4.7 Hz, 2H), 4.51 – 4.42 (m, 2H), 4.22 (dd, J = 11.9, 7.0 Hz, 2H), 3.70 (d, J = 4.8 Hz, 4H), 3.45 (t, J = 6.4 Hz, 4H), 1.53 – 1.44 (m, 4H), 1.24 (s, 8H). ^{13}C NMR (100 MHz, $CDCl_3$): δ ppm 179.65, 148.58, 147.23, 136.98, 131.16, 129.65, 129.06, 128.02, 125.31, 125.12, 123.94, 122.44, 114.84, 73.74, 72.38, 68.85, 66.34, 65.82, 30.79, 30.53, 29.94, 29.72, 29.58, 26.21.

7-(4-(Diphenylamino)phenyl)-3-(((6-((7-(4-(diphenylamino)phenyl)-5-formyl-2,3-dihydrothieno[3,4-*b*][1,4]dioxin-2-yl)methoxy)octyl)oxy)methyl)-2,3-dihydrothieno-[3,4-b][1,4]dioxine-5-carbaldehyde (4b). ^{1}H NMR (400 MHz, DMSO-d_6): δ ppm 9.83 (s, 1H), 9.82 (s, 1H), 7.68 (dd, J = 16.9, 8.8 Hz, 4H), 7.34 (td, J = 8.2, 2.7 Hz, 8H), 7.17 – 7.03 (m, 12H), 6.96 (dd, J = 8.8, 6.9 Hz, 4H), 4.63 (d, J = 4.6 Hz, 1H), 4.53 (d, J = 9.7 Hz, 2H), 4.47 (dd, J = 12.0, 2.1 Hz, 1H), 4.32 – 4.17 (m, 2H), 3.70 (t, J = 4.5 Hz, 4H), 3.45 (dd, J = 13.8, 7.3 Hz, 4H), 1.46 (dd, J = 13.1, 6.4 Hz, 4H), 1.22 (d, J = 22.0 Hz, 8H). ^{13}C NMR (100 MHz, $CDCl_3$): δ ppm 179.63, 148.54, 147.22, 137.18, 129.65, 128.01, 127.98, 125.31, 123.93, 122.44, 114.75, 73.74, 72.91, 72.39, 72.37, 69.00, 68.86, 66.94, 66.34, 29.73, 29.56, 26.20.

3,3'-((Octane-1,6-diylbis(oxy))bis(methylene))bis(7-(4-(diphenylamino)phenyl)-2,3-dihydrothieno[3,4-*b*][1,4]dioxine-5-carbaldehyde) (4c). ^{1}H NMR (400 MHz, DMSO-d_6): δ ppm 9.81 (s, 2H), 7.69 (d, J = 8.8 Hz, 4H), 7.32 (t, J = 7.8 Hz, 8H), 7.08 (dd, J = 20.4, 7.6 Hz, 12H), 6.92 (d, J = 8.7 Hz, 4H), 4.52 (d, J = 10.8 Hz, 4H), 4.25 (dd, J = 11.7, 7.7 Hz, 2H), 3.67 (d, J = 4.4 Hz, 4H), 3.41 (dd, J = 14.3, 6.9 Hz, 4H), 1.46 – 1.37 (m, 4H), 1.11 (s, 8H). ^{13}C NMR (100 MHz, $CDCl_3$): δ ppm 179.67, 148.55, 147.24, 136.98, 129.65, 127.98, 125.31, 123.94, 122.43, 77.56, 77.24, 76.93, 72.89, 72.34, 69.00, 66.92, 29.94, 29.72, 29.54, 26.19.

Synthesis of 3,3'-(2,2'-((octane-1,8-diylbis(oxy))bis(methylene))bis(7-(4-(diphenylamino)phenyl)-2,3-dihydrothieno[3,4-*b*][1,4]dioxine-5,2-diyl))bis(2-cyanoacrylic acid) (D1). Under a nitrogen atmosphere, a mixture of compound **4a** (80 mg, 0.08 mmol) and cyanoacetic acid (20 mg, 0.23 mmol) in a mixed solution of 10 mL acetonitrile and 3 mL chloroform was refluxed with the presence of piperidine (0.4 mL) for 8 h. After cooling to room temperature, the mixture was poured into water and extracted with DCM. The combined organic solution was washed with brine and dried over anhydrous sodium sulfate. After removal of the solvent, the residue was purified by flash column chromatography (silica gel, DCM/MeOH = 10/1). A red solid was obtained with a yield of 66% (60 mg). ^{1}H NMR (400 MHz, DMSO-d_6): δ ppm 8.13 (s, 2H), 7.65 (d, J = 8.6 Hz, 4H), 7.30 (t, J = 7.1 Hz, 8H), 7.06 (m, 12H), 6.91 (d, J = 8.2 Hz, 4H), 4.52 (d, J = 12.1 Hz, 4H), 4.22 (s, 4H), 3.64 (s, 6H), 1.38 (s, 4H), 1.08 (s, 8H). ^{13}C NMR (100 MHz, $CDCl_3$): δ ppm 150.04, 149.02, 146.99, 142.79, 136.92, 131.82, 129.70, 129.12, 128.39, 125.55, 124.45, 124.24, 123.71, 121.81, 109.79, 74.96, 72.34, 72.25, 68.95, 68.82, 66.05, 29.93, 29.35, 29.27, 29.20, 29.13, 25.85. HRMS (ESI, *m*/*z*): [M-H]$^-$ calcd for $C_{66}H_{57}N_4O_{10}S_2$, 1129.3516; found 1129. 3552.

Synthesis of 3-(2-(((8-((7-(2-carboxy-2-cyanovinyl)-5-(4-(diphenylamino)phenyl)-2,3-dihydrothieno[3,4-*b*][1,4]dioxin-2-yl)methoxy)octyl)oxy)methyl)-7-(4-(diphenylamino)phenyl)-2,3-dihydrothieno[3,4-*b*][1,4]dioxin-5-yl)-2-cyanoacrylic acid (D2). Compound **D2** was synthesized similarly as compound **D1** and obtained as red solid, yield 72% (70 mg). ^{1}H NMR (400 MHz, $CDCl_3$): δ ppm 8.34 (d, J = 14.7 Hz, 2H), 7.62 (d, J = 8.0 Hz, 4H), 7.27 (m, 10H), 7.08 (d, J = 7.9 Hz, 10H), 6.96 (d, J = 8.0 Hz, 4H), 4.43 (d, J = 40.1 Hz, 4H), 4.21 (d, J = 37.9 Hz, 2H), 3.85 – 3.60 (m, 4H), 3.49 (s, 4H), 1.51 (m, 8H), 1.25 (s, 4H). ^{13}C NMR (100 MHz, $CDCl_3$): δ ppm 149.64, 148.82, 147.01, 142.30, 137.09, 130.86, 129.97, 129.69, 128.33, 125.50, 124.66, 124.59, 124.16, 121.88, 109.78, 74.11, 72.83, 72.35, 68.81, 67.15, 66.38, 53.10, 29.93, 29.61, 29.41, 26.15, 26.01, 21.01. HRMS (ESI, *m*/*z*): [M-H]$^-$ calcd for $C_{66}H_{57}N_4O_{10}S_2$, 1129.3516; found 1129. 3531.

Synthesis of 3,3'-(3,3'-((octane-1,8-diylbis(oxy))bis(methylene))bis(7-(4-(diphenylamino)phenyl)-2,3-dihydrothieno[3,4-*b*][1,4]dioxine-5,3-diyl))bis(2-cyanoacrylic acid) (D3). Compound **D3** was synthesized similarly as compound **D1** and obtained as red solid, yield 70% (78 mg). ^{1}H NMR (400 MHz, $CDCl_3$): δ ppm 8.42 (s, 2H), 7.62 (s, 4H), 7.26 (s, 4H), 7.09 (s, 14H), 6.98 (s, 6H), 4.54 (s, 2H), 4.36 (d, J = 12.1 Hz, 2H), 4.13 (d, J = 9.2 Hz, 2H), 3.77 (s, 4H), 3.57 (s, 4H), 1.65 (s, 4H), 1.39 (s, 8H). ^{13}C NMR (100 MHz, $CDCl_3$): δ ppm 149.35, 148.88, 147.05, 142.50, 137.04, 130.68, 129.87, 129.66, 128.33, 125.48, 124.71, 124.37, 124.12, 121.89, 109.75, 72.81, 72.21, 68.88, 67.14, 32.15, 29.92, 29.59, 29.33, 26.05, 22.92. HRMS (ESI, *m*/*z*): [M-H]$^-$ calcd for $C_{66}H_{57}N_4O_{10}S_2$, 1129.3516; found 1129. 3513.

Synthesis of 2-(methoxymethyl)-2,3-dihydrothieno[3,4-*b*]-[1,4]dioxine (5). Compound **5** was synthesized similarly as compound **2** using methyl iodide instead of 1,8–dibromooctane and obtained as a pale yellow oily liquid, yield 79% (0.73 g). ^{1}H NMR (400 MHz, $CDCl_3$): δ ppm 6.33 (dd, J = 9.5, 3.6 Hz, 2H), 4.31 (d, J = 5.5 Hz, 1H), 4.23 (d, J = 11.7 Hz, 1H), 4.05 (dd, J = 11.6, 7.7 Hz, 1H), 3.61 (m, 2H), 3.42 (s, 3H). ^{13}C NMR (100 MHz, $CDCl_3$): δ ppm 100.02, 99.83, 72.78, 71.25, 66.30, 59.78.

Synthesis of compound 6a and 6b. Compound **6a** and **6b** was synthesized similarly as compound **3a**, **3b** and **3c**, and obtained as a pale yellow oily liquid. The crude product was purified by column chromatography on silica gel with hexane/DCM (v/v = 1/1) as eluent to remove other by-products. The obtained isomer mixture of compounds **6a** and **6b** was directly used for the next step.

Synthesis of compound 7a and 7b. Compound **7a** and **7b** was synthesized similarly as compound **4a**, **4b** and **4c**, and obtained as yellow solid. The product was purified by silica gel column chromatography with hexane/DCM (v/v = 1/1) as eluent to produce pure compounds **7a** (112 mg) and **7b** (105 mg).

7-(4-(Diphenylamino)phenyl)-2-(methoxymethyl)-2,3-dihydrothieno[3,4-*b*][1,4]dioxine-5-carbaldehyde (7a). ^{1}H NMR (400 MHz, DMSO-d_6): δ ppm 9.84 (s, 1H), 7.67 (d, J = 8.8 Hz, 2H), 7.35 (t, J = 7.8 Hz, 4H), 7.17 – 7.03 (m, 6H), 6.98 (d, J = 8.8 Hz, 2H), 4.67 (d, J = 4.9 Hz, 1H), 4.54 – 4.43 (m, 1H), 4.23 (dd, J = 12.0, 7.3 Hz, 1H), 3.69 (d, J = 4.8 Hz, 2H), 3.34 (s, 3H). ^{13}C NMR (100 MHz, DMSO-d_6): δ ppm 179.43, 150.05, 148.52, 147.13, 137.77, 130.42, 128.45, 127.83, 125.49, 125.04, 124.65, 122.45, 114.33, 74.44, 70.67, 66.29, 59.48.

7-(4-(Diphenylamino)phenyl)-3-(methoxymethyl)-2,3-dihydrothieno[3,4-*b*][1,4]dioxine-5-carbaldehyde (7b). ^{1}H NMR (400 MHz, DMSO-d_6): δ ppm 9.83 (s, 1H), 7.69 (d, *J* = 8.8 Hz, 2H), 7.35 (t, *J* = 7.8 Hz, 4H), 7.11 (dd, *J* = 18.1, 7.9 Hz, 6H), 6.96 (d, *J* = 8.8 Hz, 2H), 4.55 (d, *J* = 10.3 Hz, 2H), 4.28 (dd, *J* = 11.9, 8.0 Hz, 1H), 3.68 (t, *J* = 4.5 Hz, 2H), 3.33 – 3.30 (m, 3H). ^{13}C NMR (100 MHz, DMSO-d_6): δ ppm 179.58, 149.89, 148.52, 147.11, 137.79, 130.44, 128.33, 127.69, 125.61, 125.05, 124.72, 122.25, 114.29, 73.46, 70.79, 66.89, 59.51.

Synthesis of 2-cyano-3-(7-(4-(diphenylamino)phenyl)-2-(methoxymethyl)-2,3-dihydrothieno[3,4-*b*][1,4]dioxin-5-yl)acrylic acid (S1). Compound **S1** was synthesized similarly as compound **D1** and obtained as red solid, yield 87% (72 mg). ^{1}H NMR (400 MHz, DMSO-d_6): δ ppm 8.16 (s, 1H), 7.64 (d, *J* = 8.9 Hz, 2H), 7.33 (t, *J* = 7.9 Hz, 4H), 7.15 – 7.03 (m, 6H), 6.97 (d, *J* = 8.8 Hz, 2H), 4.66 (d, *J* = 4.9 Hz, 1H), 4.49 (d, *J* = 11.8 Hz, 1H), 4.18 (dd, *J* = 11.9, 7.6 Hz, 1H), 3.68 (d, *J* = 4.7 Hz, 2H), 3.34 (s, 3H). ^{13}C NMR (100 MHz, DMSO-d_6): δ ppm 172.68, 164.80, 149.82, 148.72, 147.02, 140.43, 137.84, 130.44, 128.58, 125.62, 124.80, 124.69, 122.31, 117.85, 108.60, 94.34, 74.79, 70.64, 66.30, 59.40. HRMS (ESI, *m*/*z*): $[M+H]^+$ calcd for $C_{30}H_{25}N_2O_5S$, 525.1484; found 525.1482.

Synthesis of 2-cyano-3-(7-(4-(diphenylamino)phenyl)-3-(methoxymethyl)-2,3-dihydrothieno[3,4-*b*][1,4]dioxin-5-yl)acrylic acid (S2). Dye isomer **S2** was synthesized similarly as compound **D1** and obtained as red solid, yield 81% (55 mg). ^{1}H NMR (400 MHz, DMSO-d_6): δ ppm 8.17 (s, 1H), 7.67 (d, *J* = 8.8 Hz, 2H), 7.34 (t, *J* = 7.8 Hz, 4H), 7.10 (dd, *J* = 18.3, 7.9 Hz, 6H), 6.96 (d, *J* = 8.8 Hz, 2H), 4.56 (d, *J* = 10.3 Hz, 2H), 4.27 (dd, *J* = 12.3, 8.3 Hz, 1H), 3.66 (t, *J* = 4.2 Hz, 2H), 3.32 (s, 3H). ^{13}C NMR (100 MHz, DMSO-d_6): δ ppm 164.78, 149.79, 148.75, 146.99, 140.67, 137.84, 130.46, 128.48, 127.86, 125.76, 124.88, 124.65, 122.08, 117.73, 108.53, 94.01, 73.57, 70.68, 67.28, 59.51. HRMS (ESI, *m*/*z*): $[M+H]^+$ calcd for $C_{30}H_{25}N_2O_5S$, 525.1484; found 525.1483.

Characterizations. UV-vis absorption spectra of dye solutions and dye-loaded films were recorded with a Shimadzu UV-2550PC spectrophotometer. Cyclic voltammetry measurements were performed with a CHI660E electrochemical workstation using a typical three-electrode electrochemical cell in a solution of tetrabutylammonium hexafluorophosphate (0.1 M) in water-free acetonitrile with a scan rate of 50 mV s^{-1} at room temperature under argon. Dye adsorbed TiO_2 on conductive glass was used as the working electrode, a Pt wire as the counter electrode, and an Ag/Ag^+ electrode as the reference electrode. The potential of the reference electrode was calibrated by ferrocene, and all potentials mentioned in this work are against normal hydrogen electrode (NHE). The film thickness was measured by a surface profiler (Veeco Dektak 150, USA).

DSSC Fabrication and Photovoltaic Measurements. TiO_2 nanoparticle (20 nm) films (12 μm) in direct contact with the FTO substrate were fabricated with a screen printing method and used in this study. The films were sintered at 500 ℃ for 2 h to achieve good necking of neighboring TiO_2 particles. The sintered films were then treated with 0.05 M $TiCl_4$ aqueous solution at 70 ℃ for 30 min followed by calcinations at 450 ℃ for 30 min. When TiO_2 electrodes were cooled down at around 120 ℃, the electrodes were dipped in dye solutions (0.3 mM in toluene) for 24 h at room temperature for complete dye adsorption. The dye-loaded TiO_2 film as working electrode and the Pt-coated FTO as counter electrode were separated by a hot-melt Surlyn film (30 μm) and sealed together by pressing them under heat. Redox electrolyte (0.6 M 1,2-dimethyl-3-*n*-propylimidazolium iodide (DMPImI), 0.1 M LiI, 0.1 M I_2, and 0.5 M 4-*tert*-butylpyridine (TBP) in acetonitrile) was introduced through a hole in the counter electrode via suction through another drilled hole. Finally, the two holes were sealed using additional hot melt Surlyn film covered with a thin glass slide. Quasi-solid-state gel electrolyte was prepared by mixing 5wt% poly(vinylidenefluoride-co-hexafluoropropylene) in a redox solution containing 0.1M LiI, 0.1 M I_2, 0.5 M TBP and 0.6 M DMPImI in 3-methoxypropionitrile (MPN) under heating until all solids were dissolved. After introducing the hot gel solution into the internal space of the cell from the two holes predrilled on the back of the counter electrode, a uniform motionless polymer gel layer was formed between the working and the counter electrodes, and then the holes were sealed with a Surlyn film covered with a thin glass slide under heat. A black mask with aperture area of 0.2304 cm^2 was used during measurement to avoid stray light. The working performance of DSSC was tested by recording the current density–voltage (*J*-*V*) curves with a Keithley 2400 source meter (Oriel) under illumination of simulated AM1.5G solar light coming from a solar simulator (Oriel-94043A equipped with a 450 W Xe lamp and an AM1.5G filter). The light intensity was calibrated using a standard Si solar cell (Newport 91150).

Results and Discussion

Synthesis of Sensitizers

The straightforward synthetic approaches to the isomeric dyes are depicted in Scheme 1. The synthetic procedure for isomers **D1**, **D2**, and **D3** started from 2-hydroxymethyl subsituted 3,4-ethylenedioxythiophene (EDOT), which was prepared according to priviously reported method.[12] Dissolving of sodium hydride to the solution of 2-hydroxymethyl subsituted EDOT in tetrahydrofuran and followed by addition of 1,8-dibromooxtane produced the EDOT bisfunctionalized bridge compound **2** (72 %). It should be noted that the resulting compound **2** contains four reactive sites with similar reactivity at the 2,5-positions on the two thiophene rings in the EDOT moieties. Therefore, after refluxing with 2 quiv. of Vilsmeier reagents,[13] three isomers (**3a**, **3b** and **3c**) containing two aldehyde groups on different thiophene rings were obtained with a ratio of around 1:1:1. The absence of the product with two aldehyde groups on the same thiophene rings is probably due to passivated thiophene ring after introduction of one aldehyde, an electron-withdrawing group. However, since the resulting isomers do not show remarkably different polarity, it is not straightforward to separate the mixture of the three isomers. Interestingly, the incorporation of two triphenylamino groups on the other two reactive sites has brought a significant difference among the product polarities. Herein, the electron donor, 4-bromo-*N*,*N*-diphenylaniline, was attached via C-H bond activation reaction[14] which has shortened the synthetic procedure by two steps. Otherwise, related bromide and boronic acid reagents have to be prepared before a Pd-catalyzed Suzuki coupling reaction. The separated isomeric compounds **4a**, **4b**, and **4c** were verified by ^{1}H NMR spectroscopy (Fig. 2). The ^{1}H NMR spectra of **D1** and **D3** display only one singlet peak at δ = 9.82 ppm and 9.81 ppm, respectively, assigning to the protons in the two aldehyde groups, which suggests a symmetric chemical structure in the organic dye molecules. While in the ^{1}H NMR spectrum of **D2**, two singlet peaks at δ = 9.83 and 9.82 ppm indicate that the chemical structure is asymmetric and therefore the signals for the two protons in the aldehyde groups are differed. To further specify the two isomers **D1** and **D3**,

single branched isomers **S1** and **S2** are synthesized similar to those double branched dye isomers (Scheme 2). As shown in Fig. 2, the precursors **7a** and **7b** exhibit different proton signals in the δ region from 4.7 to 4.0 ppm, which are assigned to the three protons on the dioxane ring of EDOT unit. The chemical shift of Ha for compound **7a** moves to the lower field as compared with that for compound **7b**, since Ha is closer to the cyanoacrylic acid, an electron-withdrawing group. Similar phenomena can be also observed for double branched precursors **4a** and **4c** (Fig. 2). In the last step, the obtained precursors were converted to the corresponding dye isomers by Knoevenagel condensation[15] with the presence of cyanoacetic acid and piperidine. All the target compounds were characterized by ^{1}H NMR, ^{13}C NMR spectroscopy, and mass spectroscopy, and were found to be consistent with the proposed structures.

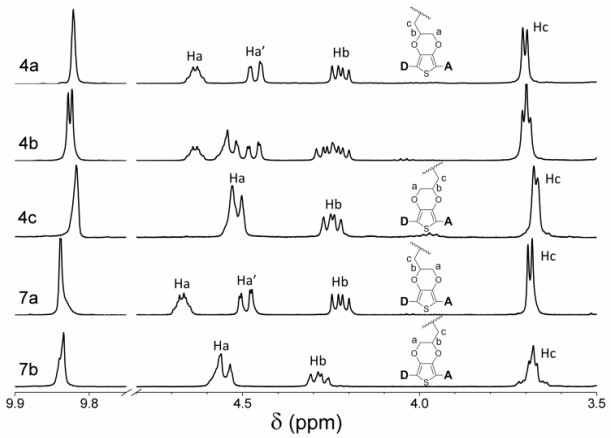

Fig. 2 ^{1}H NMR spectra of isomeric dye precursors **4a**, **4b**, **4c**, **7a**, and **7b**.

Photophysical Properties

The photophysical characteristics of the resulting dye isomers were investigated by UV–vis absorption spectra in dilute chloroform solutions and on TiO_2 films at room temperature. The UV-vis absorption spectra of the three isomeric dyes are shown in Fig. 3 and the corresponding photophysical data are summarized in Table 1. In chloroform solutions, all the dyes exhibit two distinct absorption bands (Fig. 3a). The absorption band in the high-energy region (< 400 nm) corresponds to the π–π* electron transitions of the conjugated backbone, and the other relatively stronger absorption band in the low-energy region (> 400 nm) can be assigned to the intramolecular charge transfer (ICT) from the electron donating unit to the electron-withdrawing group. Such intense ICT band is unlike our previously reported double D-π-A system,[10a] where the ICT band is much weaker than the other band for π–π* transitions. This is probably due to their different bridge linking the two D-π-A branches. In our previously reported dye **FNE92**, the crossed two branches are linked by a conjugated thiophene bridge. The twisted conjugation structure may affect the effective conjugation and the ICT interactions. Herein, the two D-π-A branches are connected by a flexible octyloxy chain which has little influence on the electronic structures of the dye molecules. Under the same condition, the three isomers (**D1**, **D2** and **D3**) exhibit the absorption maximum at 501, 494, 488 nm. To explain the absorption difference among these dye isomers, the absorption spectra of the single D-π-A branched dye isomers **S1** and **S2** were investigated. As shown in Fig. 3a, isomer **S1** displays the maximum absorption wavelength at 496 nm, while isomer **S2** demonstrates the maximum absorption wavelength at 491 nm with a slight hypsochromic shift of 5 nm. Since the only structural difference of the two isomers is the substituted position of the methoxymethyl group on EDOT unit, the slight absorption difference is stemmed from substituted methoxymethyl group at 3- or 4-position of EDOT unit. As the substituted methoxymethyl group is far away from the conjugation backbone of the dye molecule, the absorption shift is probably due to the changed electron density on the two oxygen atoms in EDOT unit which is indirectly affected by the introduced methoxymethyl group. Therefore, the hypsochromic shift of the absorption maximum from **D1** to **D2**, and further to **D3**, can be similarly explained and originate from the bridged octyloxy groups attach at different position on EDOT units, which affects the lone pair electrons of the two oxygen atoms and thus the π-conjugation structure. This speculation is further proved by theoretical calculation as discussed below. To further investigate the different intermolecular interactions, the UV-vis absorption spectra of the dye solutions with different concentration were recorded. As shown in Fig. S1-S5, when the concentration increases from 10^{-6} M to 10^{-4} M, no obvious difference can be found for the absorption maxima of double branched dye isomers **D1**, **D2**, and **D3**, while a bathochromic shift of 9 and 6 nm can be observed for the absorption maximum of single branched dye isomers **S1** and **S2**, respectively. These results indicate that the double branched structure has effectively inhibited the interactions among the D-π-A branches.

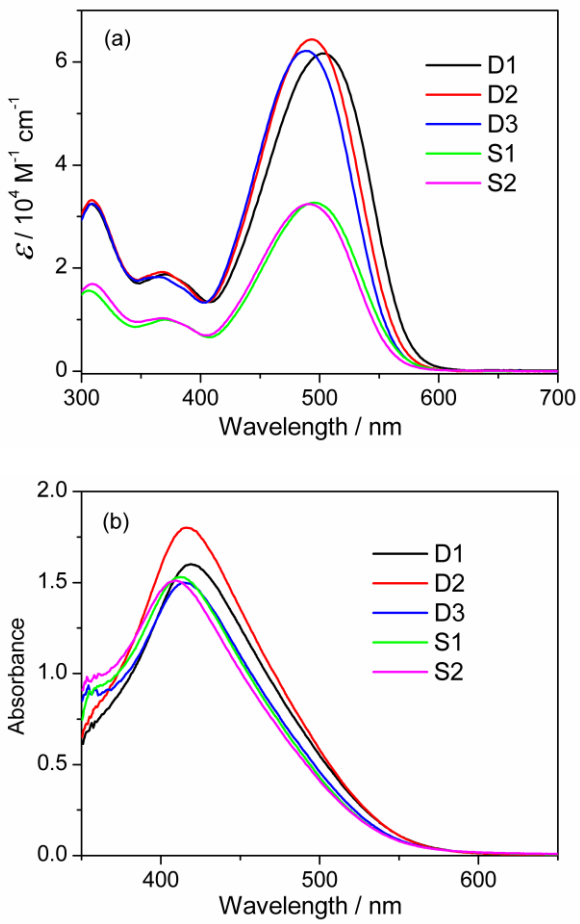

Fig. 3 UV-vis absorption spectra of the dye isomers (a) in chloroform solutions and (b) on TiO_2 films (3 μm).

Table 1. UV-vis absorption and electrochemical properties of dye isomers **D1**, **D2**, **D3** and references **S1**, **S2**.

Dye	Absorption			HOMO[b]	$E_{0\text{-}0}$	LUMO[b]
	λ_{max}[a] nm	ε[a] M^{-1} cm^{-1}	λ_{max} on TiO_2 nm	V	eV	V
D1	501	6.16×10^4	419	1.13	2.29	-1.16
D2	494	6.43×10^4	416	1.14	2.30	-1.16
D3	488	6.21×10^4	414	1.17	2.31	-1.14
S1	496	3.27×10^4	412	1.10	2.33	-1.23
S2	491	3.24×10^4	410	1.12	2.33	-1.21

[a] Absorption peaks (λ_{max}) and molar extinction coefficients (ε) were measured in toluene solutions (~5×10^{-6} M). [b] The potentials (*vs.* NHE) were calibrated with ferrocene.

The UV-vis absorption spectra of the organic dye isomers anchored on transparent mesoporous TiO_2 films were also measured and shown in Fig. 3b. Similarly, a slight hypsochromic shift can be observed for double D-π-A branched organic dye isomers from **D1** to **D2**, and further to **D3**. This is consistent with the absorption spectra in chloroform solutions and originates from their different chemical structures. Moreover, upon the adsorption of the organic dye isomers on the surface of the TiO_2 films, a significant hypsochromic shift of 74~81 nm with respect to those in solutions can be observed, which is owing to the deprotonation of the carboxylic acid. Such hypsochromic shift of the absorption spectra for organic dyes adsorbed on the TiO_2 films has also been observed in other metal-free organic dyes.[16]

Dye Adsorption

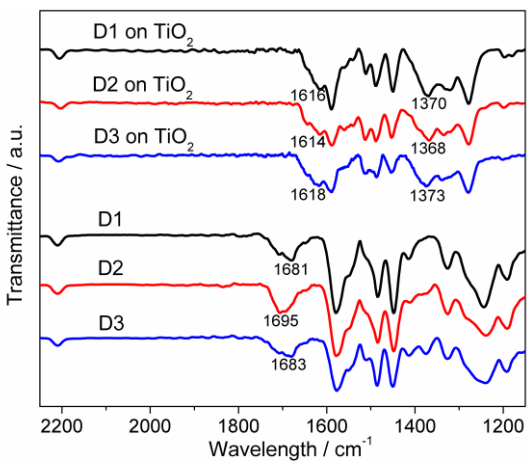

Fig. 4 IR spectra of the isomeric dye powders and stained TiO_2 films.

The anchoring properties of the isomeric dyes on the TiO_2 films were characterized by measuring the IR spectra of the dye powders and dye-loaded TiO_2 films. A stretching band at around 2216 cm^{-1}, assigning to the stretching vibration of C≡N group,[17] can be observed for all the double D-π-A branched dye powders and dye-loaded TiO_2 films (Fig. 4). However, the carbonyl peaks at 1681, 1695, and 1683 cm^{-1} for isomers **D1**, **D2**, and **D3**, respectively, disappeared after anchoring on TiO_2 films, while another peaks appeared in the IR spectra (Fig. 4) for the asymmetric (1616, 1614, and 1618 cm^{-1}) and symmetric (1370, 1368, and 1373 cm^{-1}) of carboxylate groups.[18] The results suggest that all the double D-π-A branched dye isomers were chemically adsorbed onto the TiO_2 film via double-anchoring modes. Therefore, according to the Deacon Philips rule[19] and previous similar report,[18,20] the dye molecules most likely adsorb on the TiO_2 surface via a bidentate bridging binding mode.

Electrochemical Properties.

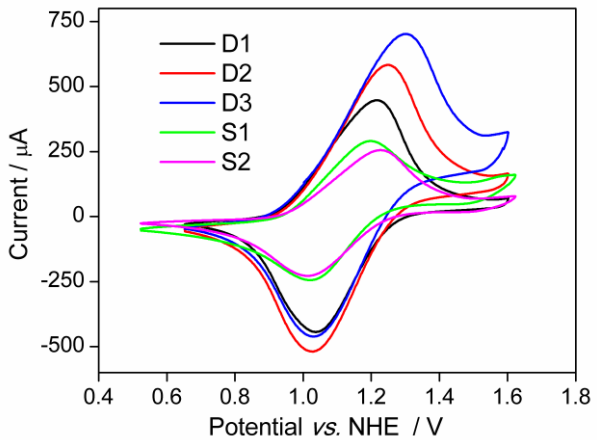

Fig. 5 Cyclic voltammograms of the isomeric dye-loaded TiO_2 films.

To study the possibility of the photo-generated electron injection and the sensitizer regeneration, CV was carried out in a typical three-electrode electrochemical cell with TiO_2 films stained with sensitizer as the working electrode in a solution of tetrabutylammonium hexafluorophosphate (0.1 M) in water-free acetonitrile with a scan rate of 50 mV s^{-1}.The highest occupied molecular orbital (HOMO) levels of dyes **D1**, **D2**, and **D3**, taken from the first oxidation half-wave potential, are determined to be 1.13, 1.14, and 1.17 V (*vs.* normal hydrogen electrode, NHE, the same below), respectively, which are more positive than the redox potential of the I^-/I_3^- redox couple (~0.4 V), indicating that the reduction of the oxidized dyes with I^- ions is thermodynamically feasible.[21] Correspondingly, calculated from HOMO levels and the optical band gap derived from the wavelength at 10% maximum absorption intensity for the dye-loaded TiO_2 film,[22] the lowest unoccupied molecular orbital (HOMO) energy levels of dyes **D1**, **D2**, and **D3** are calculated to be -1.16, -1.16, and -1.14 V, respectively, indicating enough driving force of the electron injection from their excited states to TiO_2 films.[21] The energy levels for the

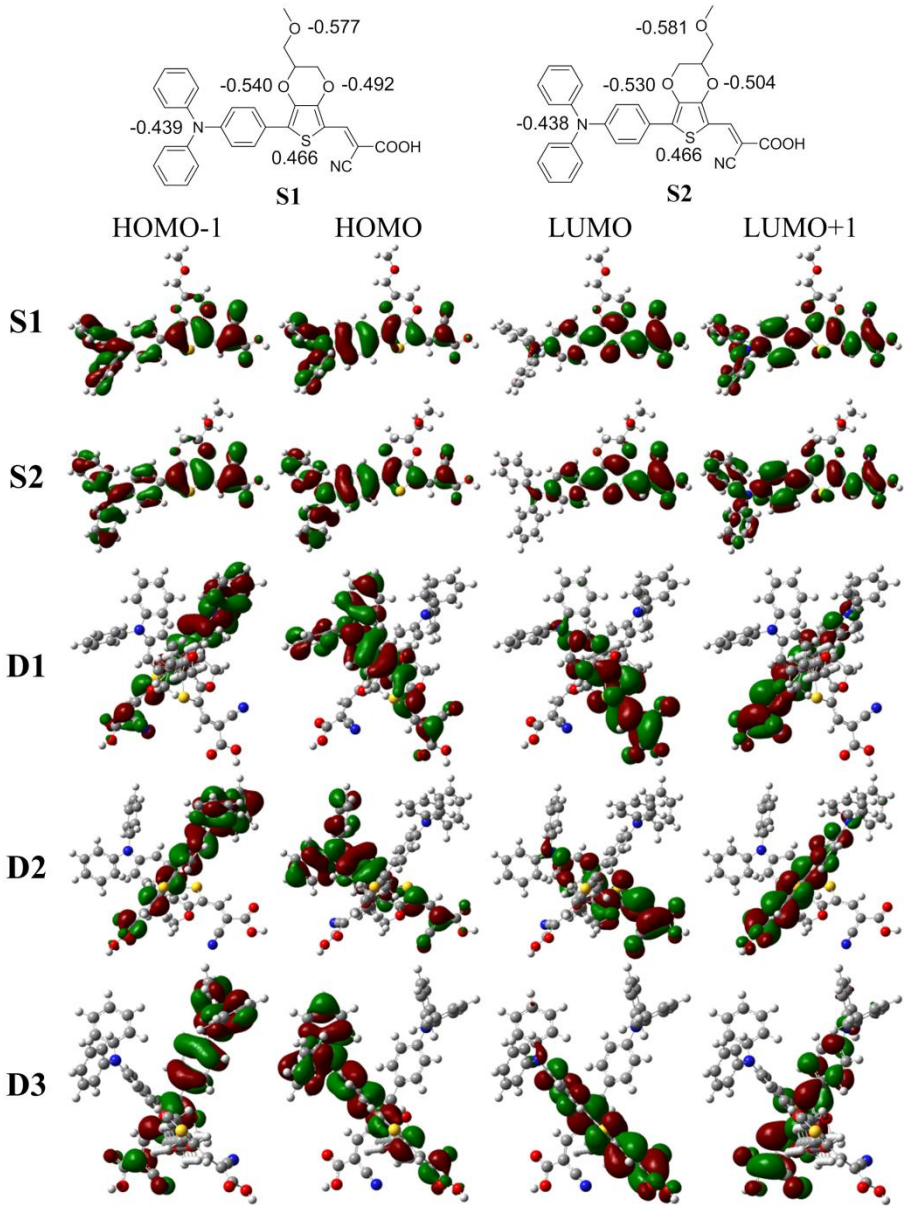

Fig. 6 Calculated atomic charges of references **S1** and **S2** and frontier molecular orbitals for the dye isomers.

resulting organic dyes are summarized in Table 1. The similar HOMO/LUMO values of **D1**, **D2**, and **D3** are not difficult to be understood since all of the dye isomers have identical electron donors and acceptors except for the octyloxy bridge substituted at different position on the EDOT unit.

Theoretical Approach

To investigate the geometrical structures and electronic properties of the organic dye isomers, density functional calculations were conducted with the Gaussian 03 program using B3LYP method and 6-31G* basis set.[23] To explain the different absorption properties for the related dye isomers, the Natural Bond Orbital (NBO) population analysis[24] is utilized to compare the charge distribution on the EDOT unit. As shown in Fig. 6, the NBO charge for the two oxygen atoms on EDOT unit in isomeric dye **S1** is -0.540 and -0.492, respectively. However, when the substituted methoxymethyl group is removed from left to right, the NBO charge for the two related oxygen atoms in isomeric dye **S2** is calculated to be -0.530 and -0.504, respectively, which is the most significant change for the atom charge when the dye isomer shifts from **S1** to **S2**. These results suggest that when substituted position of the alkyl group on the EDOT unit changes, the charge distribution on the two oxygen atoms are different, which results in the varied π-conjugation and ICT interactions. Similar effect can be also observed for the double branched dye isomers **D1**, **D2**, and **D3**. This well explains their slightly different absorption behavior (Fig. 3).

For reference dyes **S1** and **S2** with rigid single branch, the HOMO distributes along the whole conjugated system and the LUMO delocalizes over the cyanoacrylic acid group through conjugated bridge, facilitating electron transfer from the electron-donating moiety to the electron-withdrawing moiety and further to the CB of TiO_2 via the carboxylate anchoring

group.[25] For double branched dye isomers **D1**, **D2**, and **D3**, the two rod-type branches cross perpendicularly, which not only interrupts the interactions between the two intramolecular D-π-A branches but also weakens the intermolecular interactions among the organic dye isomers, which is beneficial to the DSSC performance. Moreover, it can be found that for all the double branched dye isomers, the HOMO and the LUMO delocalize over the same D-π-A branch, while the HOMO-1 and the LUMO+1 delocalize over the other D-π-A branch. Upon excitation by the sunlight, the excited electrons can easily transfer on two separated branches from the donor to the acceptor and further to TiO_2.

Solar Cell Performance

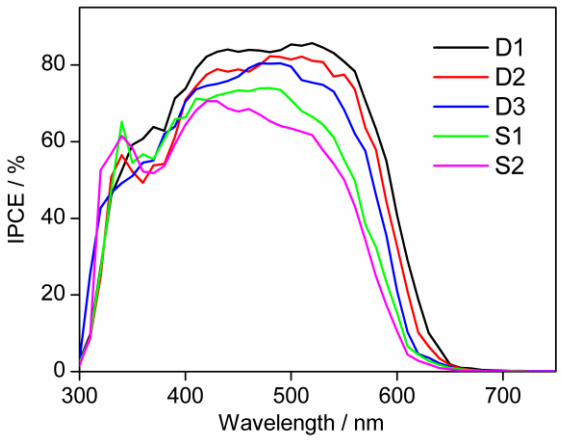

Fig. 7 IPCE spectra for the DSSCs based on the dye isomers with liquid electrolyte.

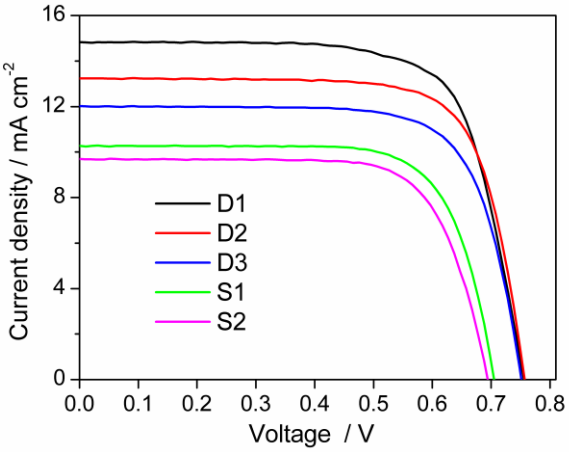

Fig. 8 *J* - *V* curves for the DSSCs based on the dye isomers with liquid electrolyte.

The DSSCs based on the dye isomers were fabricated using a liquid electrolyte (0.6 M 1,2-dimethyl-3-*n*-propylimidazolium iodide (DMPImI), 0.1 M LiI, 0.1 M I_2, and 0.5 M 4-*tert*-butylpyridine (TBP) in acetonitrile). Action spectra of the incident photon-to-current conversion efficiencies (IPCE) as a function of incident wavelength for DSSCs based on the organic dye isomers are shown in Fig. 7. The highest IPCE values are over 80% for all the DSSCs based on double D-π-A branched organic dye isomers, and around 70% for the DSSCs based on single D-π-A branched organic dye isomers. According to the formula, IPCE(λ) = LHE(λ) × Φ_{inj} × Φ_c,[26] where LHE(λ) is the light-harvesting efficiency, Φ_{inj} is the electron injection efficiency, and Φ_c is the charge collection efficiency, since all the dye isomers have similar HOMO and LUMO energy levels, the different IPCE values for the two types of organic dyes may result from their different charge injection efficiency. For single branched dye isomers **S1** and **S2**, the rod-like D-π-A branches tend to pack with each other and therefore self-quench their excited states, which results in the reduced electron injection efficiencies and lower IPCE values as compared with those for double branched dye isomers. Moreover, the IPCE spectrum becomes broader when the dye isomer shifts from **D3** to **D2** and further to **D1**, which is in good agreement with their absorption spectra on TiO_2 films.

Table 2 Photovoltaic performance of the isomeric dye based DSSCs with liuqid or quasi-solid-state electrolyte.

Electrolyte	Dye	V_{oc} mV	J_{sc} mA cm^{-2}	*FF* %	η %
Liquid	**D1**	755	14.83	72	8.1
	D2	756	13.21	75	7.5
	D3	752	12.00	73	6.6
	S1	705	10.27	73	5.3
	S2	694	9.69	73	4.9
Quasi-solid-state	**D1**	737	13.24	71	6.9
	D2	731	11.94	70	6.1
	D3	736	11.55	68	5.8
	S1	696	9.60	68	4.5
	S2	683	8.65	68	4.0

The photovoltaic characteristics of the DSSCs based on the dye isomers with liquid electrolyte were evaluated under 100 mW cm^{-2} simulated AM1.5G solar light. Fig. 8 demonstrates the *J*–*V* curves for the DSSCs and the detailed photovoltaic parameters are listed in Table 2. The DSSC based on isomer **S1** produces a η of 5.3% (J_{sc}= 10.27 mA cm^{-2}, V_{oc} = 705 mV, *FF* = 0.73), while isomer **S2** based DSSC provides a slightly decreased η of 4.9% (J_{sc} = 9.69 mA cm^{-2}, V_{oc} = 694 mV, *FF* = 0.73). However, when the two rigid D-π-A branches are connected, the DSSC device incorporating double branched dye isomer gives a dramatically improved η of 8.1% for **D1** (J_{sc}= 14.83 mA cm^{-2}, V_{oc} = 755 mV, *FF* = 0.72), 7.5% for **D2** (J_{sc}= 13.21 mA cm^{-2}, V_{oc} = 756 mV, *FF* = 0.75), and 6.6% for **D3** (J_{sc} = 12.00 mA cm^{-2}, V_{oc} = 752 mV, *FF* = 0.73), respectively. It can be found that for the DSSCs based on the double D-π-A branched organic dye isomers, both J_{sc} and V_{oc} values significantly increase as compared with those for the DSSCs based on the dye isomers with single D-π-A branch. Since both single and double branched dye isomer loaded TiO_2 films have similar absorbance and energy levels, their different J_{sc} values are due to their different charge injection efficiencies. The stronger intermolecular interactions among the single branched dye molecules facilitate the self-quenching of the excited electrons. While the separated double branches in isomers **D1**, **D2**, and **D3** have weakened the intermolecular interactions and minimized the current loss from self-quenching. Moreover, the slightly different J_{sc} values among dye DSSCs based on isomers **D1**, **D2**, and **D3** are stemmed from their different absorption properties, which is consistent with the IPCE trend as shown in Fig. 7. For the other performance parameter, the higher V_{oc} values for the

DSSCs based on the double branched dye isomers can be explained by their different charge recombination rates.

To explain the V_{oc} difference among the DSSCs based on the dye isomers, the electron lifetime[27] against charge density[28] for the DSSCs was investigated. The electron lifetime was measured with controlled intensity modulated photovoltage spectroscopy (IMVS)[29] and obtained from the frequency at the top of the semicircle (f_{min}) by the relation $\tau = (2\pi f_{min})^{-1}$. As shown in Fig. 9, the electron lifetime for all the DSSCs decreases with charge density following a power law relation with the same slope, suggesting the same charge recombination mechanism in the DSSCs. Additionally, at fixed charge density, the electron lifetimes for the DSSC based on isomers **D1**, **D2**, and **D3** are very similar, while the electron lifetimes for the DSSC based on isomer **S1** and **S2** are also almost identical. This is not difficult to be understood since the two series of dye isomers have very close chemical structures, which results in the similar intermolecular interactions and charge recombination rates. However, the electron lifetime for the DSSC based on double D-π-A branched dye isomer is around 3-fold longer than that for the DSSC based on single D-π-A branched dye isomer. The cross structures of the double branched dye isomers not only weaken the intermolecular interactions and thus reduces the self-quenching of the excited state, but also block the triiodides approaching the TiO_2 surface, resulting in the enhanced electron lifetime at the same charge density. Therefore, the decreased charge recombination rate reduces electron loss at an open circuit. When more charge is accumulated in TiO_2, the Fermi level moves upward and V_{oc} gets larger, which explains the different V_{oc} values in Fig. 8.

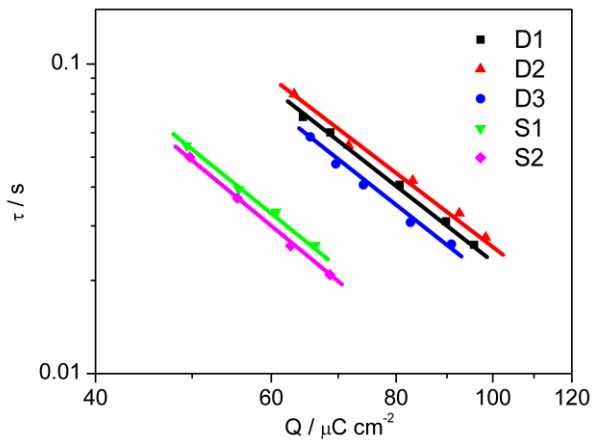

Fig. 9 Electron lifetime as a function of charge density at open circuit for the isomeric dye based DSSCs.

Compared with liquid electrolyte based DSSCs, quasi-solid-state DSSCs[30] have also attracted great attention since they there is less or no possibility for leakage of the electrolyte and thus they have shown greatly improved long-term stability. Therefore, quasi-solid-state DSSCs based on the organic dye isomers were fabricated using a quasi-solid-state gel electrolyte containing 0.1 M LiI, 0.1 M I_2, 0.5 M TBP, 0.6 M DMPImI, and 5wt% poly(vinylidenefluoride-co-hexafluoropropylene) in 3-methoxypropionitrile (MPN). The *J* - *V* curves for the quasi-solid-state DSSCs are shown in Fig. 10 and the photovoltaic parameters are summarized in Table 2. It can be found that the photovoltaic performance of the quasi-solid-state DSSCs based on the organic dye isomers is consistent with the trend for the DSSCs with liquid electrolyte discussed above. A highest efficiency of 6.9% is also achieved for isomer **D1** based quasi-solid-state DSSC under simulated AM1.5G solar irradiation

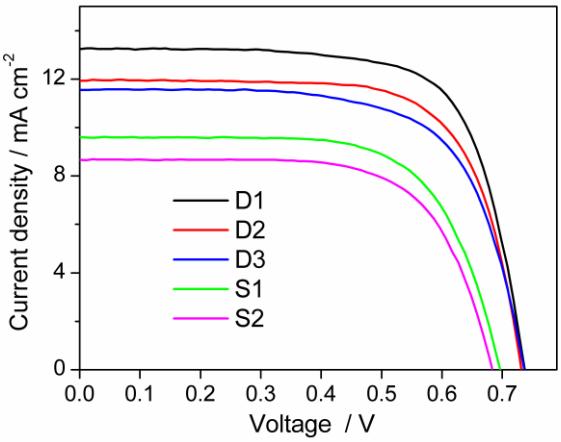

Fig. 10 *J* - *V* curves for the DSSCs based on the dye isomers with quasi-solid-state electrolyte.

Conclusions

In summary, we have designed and synthesized three double D-π-A branched organic dye isomers with octyloxy bridge linked at different positions. Compared with the reference dye isomers with single D-π-A branch, the double D-π-A branched dye isomers consisting of two separated light-harvesting moieties in one molecule are favorable for photocurrent generation. Most importantly, the double D-π-A branched organic dye isomers exhibit cross structure, which not only interrupts the interactions between the two intramolecular D-π-A branches but also weakens the intermolecular interactions among the organic dye isomers. Consequently, the charge recombination is minimized in the DSSCs based on double branched dye isomers, which results in both improved J_{sc} and V_{oc} values. Interestingly, due to the different substituted positions of the octyloxy bridge, three double D-π-A branched organic dye isomers display slightly different photophysical and photovoltaic properties. A highest power conversion efficiency of 8.1% and 6.9% is achieved for isomer **D1** based DSSC with liquid and quasi-solid-state electrolyte, respectively.

Acknowledgements

This work was financially supported by the National Basic Research Program of China (2011CB933302), the National Natural Science Foundation of China (51273045, 21201037), NCET-12-0122, STCSM (12JC1401500), Shanghai Leading Academic Discipline Project (B108), and Jiangsu Major Program (BY2010147).

Notes and references

[a] Department of Chemistry & Lab of Advanced Materials, Collaborative Innovation Center of Chemistry for Energy Materials, Fudan University, Shanghai 200438, P. R. China.

[b] College of Chemistry & Chemical Engineering, Fuyang Normal College, Fuyang, Anhui 236037, P. R. China.

1 (a) B. O'Regan and M. Grätzel, *Nature*, 1991, **353**, 737; (b) K. C. D. Robson, K. Hu, G. J. Meyer and C. P. Berlinguette, *J. Am. Chem. Soc.*, 2013, **135**, 1961; (c) E. Maggio, N. Martsinovich and A. Troisi, *Angew. Chem. Int. Ed.*, 2013, **52**, 973; (d) S. Mathew, A. Yella, P. Gao, R. Humphry-Baker, B. F. E. Curchod, N. Ashari-Astani, I. Tavernelli, U. Rothlisberger, M. K. Nazeeruddin and M. Grätzel, *Nature Chem.*, 2014, **6**, 242; (e) L.-L. Tan, J.-F. Huang, Y. Shen, L.-M. Xiao, J.-M. Liu, D.-B. Kuang and C.-Y. Su, *J. Mater. Chem. A*, 2014, **2**, 8988; (f) S. Cai, X. Hu, Z. Zhang, J. Su, X. Li, A. Islam, L. Han and H. Tian, *J. Mater. Chem. A*, 2013, **1**, 4763.

2 A. Yella, H. W. Lee, H. N. Tsao, C. Yi, A. K. Chandiran, M. K. Nazeeruddin, E. W. G. Diau, C. Y. Yeh, S. M. Zakeeruddin and M. Grätzel, *Science*, 2011, **334**, 629.

3 (a) A. Mishra, M. K. R. Fischer and P. Bäuerle, *Angew. Chem. Int. Ed.*, 2009, **48**, 2474; (b) M. Liang and J. Chen, *Chem. Soc. Rev.*, 2013, **42**, 3453; (c) Y. Wu and W. Zhu, *Chem. Soc. Rev.*, 2013, **42**, 2039.

4 (a) M. Zhang, Y. Wang, M. Xu, W. Ma, R. Li and P. Wang, *Energy Environ. Sci.*, 2013, **6**, 2944; (b) J. Yang, P. Ganesan, J. Teuscher, T. Moehl, Y. J. Kim, C. Yi, P. Comte, K. Pei, T. W. Holcombe, M. K. Nazeeruddin, J. Hua, S. M. Zakeeruddin, H. Tian and M. Grätzel, *J. Am. Chem. Soc.*, 2014, **136**, 5722.

5 (a) K. Hara, Y. Dan-oh, C. Kasada, Y. Ohga, A. Shinpo, S. Suga, K. Sayama and H. Arakawa, *Langmuir*, 2004, **20**, 4205; (b) Z.-S. Wang, Y. Cui, Y. Dan-oh, C. Kasada, A. Shinpo and K. Hara, *J. Phys. Chem. C*, 2007, **111**, 7224; (c) H. Kusama and K. Sayama, *J. Phys. Chem. C*, 2012, **116**, 23906.

6 (a) N. Koumura, Z.-S. Wang, S. Mori, M. Miyashita, E. Suzuki and K. Hara, *J. Am. Chem. Soc.*, 2006, **128**, 14256; (b) J.-H. Yum, D. P. Hagberg, S.-J. Moon, K. M. Karlsson, T. Marinado, L. Sun, A. Hagfeldt, M. K. Nazeeruddin and M. Grätzel, *Angew. Chem. Int. Ed.*, 2009, **48**, 1576.

7 (a) D. Cao, J. Peng, Y. Hong, X. Fang, L. Wang and H. Meier, *Org. Lett.*, 2011, **13**, 1610; (b) Y. Hong, J.-Y. Liao, J. Fu, D.-B. Kuang, H. Meier, C.-Y. Su and D. Cao, *Dyes Pigm.*, 2012, **94**, 481.

8 D. Heredia, J. Natera, M. Gervaldo, L. Otero, F. Fungo, C.-Y. Lin and K.-T. Wong, *Org. Lett.*, 2010, **12**, 12.

9 Y. Hong, J.-Y. Liao, D. Cao, X. Zang, D.-B. Kuang, L. Wang, H. Meier and C.-Y. Su, *J. Org. Chem.*, 2011, **76**, 8015.

10 (a) X. Ren, S. Jiang, M. Cha, G. Zhou and Z.-S. Wang, *Chem. Mater.*, 2012, **24**, 3493; (b) X. Lu, X. Jia, Z.-S. Wang and G. Zhou, *J. Mater. Chem. A*, 2013, **1**, 9697.

11 Q. Feng, Q. Zhang, X. Lu, H. Wang, G. Zhou and Z.-S. Wang, *ACS Appl. Mater. Interfaces*, 2013, **5**, 8982.

12 A. Lima, P. Schottland, S. Sadki and C. Chevrot, *Synth. Met.*, 1998, **93**, 33.

13 (a) V. J. Majo and P. J. Perumal, *J. Org. Chem.*, 1996, **61**, 6523; (b) O. Meth-Cohn and M. Ashton, *Tetrahedron Lett.*, 2000, **41**, 2749.

14 D. J. Schipper and K. Fagnou, *Chem. Mater.*, 2011, **23**, 1594.

15 S. Wade and H. Suzuki, *Tetrahedron Lett.*, 2003, **44**, 339.

16 (a) T. Kitamura, M. Ikeda, K. Shigaki, T. Inoue, N. A. Anderson, X. Ai, T. Lian and S. Yanagida, S. *Chem. Mater.*, 2004, **16**, 1806; (b) K. Hara, Z.-S. Wang, T. Sato, A. Furube, R. Katoh, H. Sugihara, Y. Dan-Oh, C. Kasada, A. Shinpo and S. J. Suga, *Phys. Chem. B*, 2005, **109**, 15476; (c) D. P. Hagberg, T. Edvinsson, T. Marinado, G. Boschloo, A. Hagfeldt and L. C. Sun, *Chem. Commun.*, 2006, 2245; (d) S.-L. Li, K.-J. Jiang, K.-F. Shao and L.-M. Yang, *Chem. Commun.*, 2006, 2792.

17 A. Abbotto, N. Manfredi, C. Marinzi, F. D. Angelis, E. Mosconi, J.-H. Yum, X. Zhang, S. M. Zakeeruddin and M. Grätzel, *Energy Environ. Sci.*, 2009, **2**, 1094.

18 H. Tian, X. Yang, R. Chen, R. Zhang, A. Hagfeldt and L. Sun, *J. Phys. Chem. C*, 2008, **112**, 11023.

19 G. B. Deacon and R. J. Phillips, *Coord. Chem. Rev.*, 1980, **33**, 227.

20 X. Jiang, K. M. Karlsson, E. Gabrielsson, E. M. J. Johansson, M. Quintana, M. Karlsson, L. Sun, G. Boschloo and A. Hagfeldt, *Adv. Funct. Mater.*, 2011, **21**, 2944.

21 A. Hagfeldt and M. Grätzel, *Chem. Rev.*, 1995, **95**, 49.

22 A. Hagfeldt, G. Boschloo, L. Sun, L. Kloo and H. Pettersson, *Chem. Rev.*, 2010, **110**, 6595.

23 M. J. Frisch, G. W. Trucks, H. B. Schlegel, G. E. Scuseria, M. A. Robb, J. R. Cheeseman, J. A. Montgomery, J. T. Vreven, K. N. Kudin, J. C. Burant, J. M. Millam, S. S. Iyengar, J. Tomasi, V. Barone, B. Mennucci, M. Cossi, G. Scalmani, N. Rega, G. A. Petersson, H. Nakatsuji, M. Hada, M. Ehara, K. Toyota, R. Fukuda, J. Hasegawa, M. Ishida, T. Nakajima, Y. Honda, O. Kitao, H. Nakai, M. Klene, X. Li, J. E. Knox, H. P. Hratchian, J. B. Cross, V. Bakken, C. Adamo, J. Jaramillo, R. Gomperts, R. E. Stratmann, O. Yazyev, A. J. Austin, R. Cammi, C. Pomelli, J. W. Ochterski, P. Y. Ayala, K. Morokuma, G. A. Voth, P. Salvador, J. J. Dannenberg, V. G. Zakrzewski, S. Dapprich, A. D. Daniels, M. C. Strain, O. Farkas, D. K. Malick, A. D. Rabuck, K. Raghavachari, J. B. Foresman, J. V. Ortiz, Q. Cui, A. G. Baboul, S. Clifford, J. Cioslowski, B. B. Stefanov, G. Liu, A. Liashenko, P. Piskorz, I. Komaromi, R. L. Martin, D. J. Fox, T. Keith, M. A. Al-Laham, C. Y. Peng, A. Nanayakkara, M. Challacombe, P. M. W. Gill, B. Johnson, W. Chen, M. W. Wong, C. Gonzalez and J. A. Pople, *Gaussian03*, revision C.02, Gaussian Inc., Wallingford, CT, 2004.

24 A. E. Reed, L. A. Curtiss and F. Weinhold, *Chem. Rev.*, 1988, **88**, 899.

25 J. Luo, M. Xu, R. Li, K.-W. Huang, C. Jiang, Q. Qi, W. Zeng, J. Zhang, C. Chi, P. Wang and J. Wu, *J. Am. Chem. Soc.*, 2014, **136**, 265.

26 Y. Chiba, A. Islam, R. Komiya, N. Koide and L. Han, *Appl. Phys. Lett.*, 2006, **88**, 223505.

27 (a) M. Miyashita, K. Sunahara, T. Nishikawa, Y. Uemura, N. Koumura, K. Hara, A. Mori, T. Abe, E. Suzuki and S. Mori, *J. Am. Chem. Soc.*, 2008, **130**, 17874; (b) B. O'Regan, K. Walley, M. Juozapavicius, A. Anderson, F. Matar, T. Ghaddar, S. M. Zakeeruddin, C. Klein and J. R. Durrant, *J. Am. Chem. Soc.*, 2009, **131**, 3541.

28 N. Kopidakis, N. R. Neale and A. J. Frank, *J. Phys. Chem. B*, 2006, **110**, 12485.

29 N. W. Duffy, L. M. Peter, R. M. G. Rajapakse and K. G. U. Wijayantha, *J. Phys. Chem. B*, 2000, **104**, 8916.

30 (a) Y. Shi, C. Zhu, L Wang, C. Zhao, W. Li, K. K. Fung, T. Ma, A. Hagfeldt and N. Wang, *Chem. Mater.*, 2013, **25**, 1000; (b) Z. Yu, D. Qin, Y. Zhang, H. Sun, Y. Luo, Q. Meng and D. Li, *Energy Environ. Sci.*, 2011, **4**, 1298; (c) J.-J.Kim, H. Choi, J.-W. Lee, M.-S. Kang, K. Song, S. O. Kang and J. Ko, *J. Mater. Chem.*, 2008, **18**, 5223; (d) Y. Shibata, T. Kato, T. Kado, R. Shiratuchi, W. Takashima, K. Kanetoa and S. Hayase, *Chem. Commun.*, 2003, **39**,

2730; (e) P. Wang, S. M. Zakeeruddin, J. E. Moser, M. K. Nazeeruddin, T. Sekiguchi and M. Grätzel, *Nat. Mater.*, 2003, **2**, 402.

Table of Contents Entry

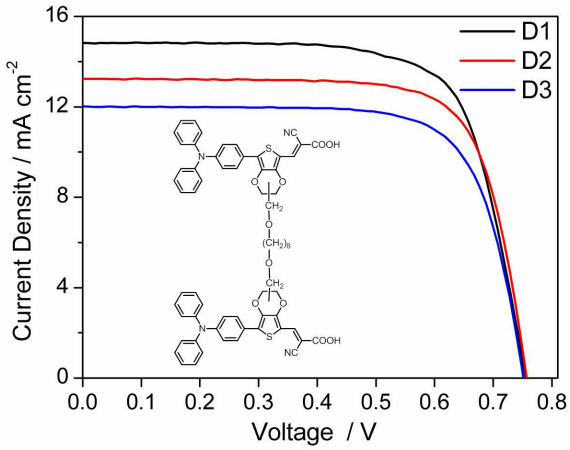

Three double D-π-A branched organic dye isomers with octyloxy bridge linked at different positions have been constructed for DSSCs.